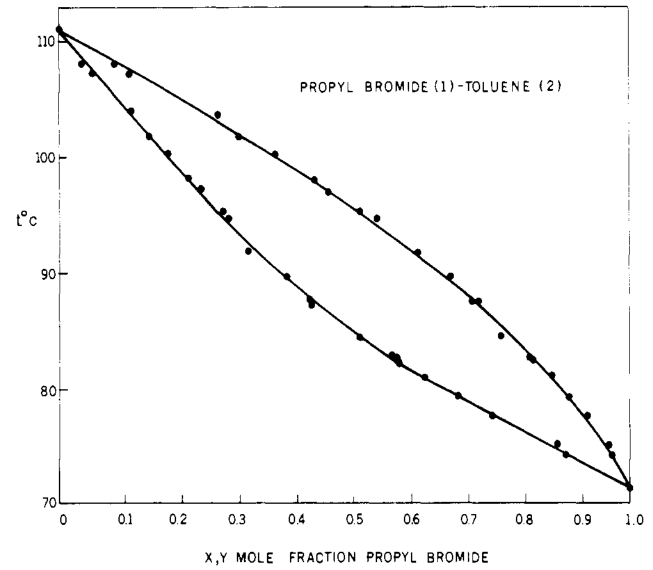

Figure 1. Boiling points diagram.

Acknowledgment

Yehudit Reizner and Moshe Golden helped in the experimental and numerical calculations.

Glossary

α, β, δ	constants
B_{ii}, B_{ij}	virial coefficient
n	number of experimental points
P	overall pressure, mmHg
P_i^0	vapor pressure of pure component, mmHg
R	gas constant
rmsd	root mean square deviation $[\sum(T_{\text{exptl}} - T_{\text{calcd}})^2]^{1/2}/n$
t, T	temperature, °C, K
V^L_i	molar volume of pure liquid i, mL/mol
x_i, y_i	molar fraction of component i in the liquid and vapor phases
γ_i	activity coefficient of component i

Subscripts

calcd	calculated
exptl	experimental
i, j, k	component i, j, k

Registry No. Propyl bromide, 106-94-5; toluene, 108-88-3.

Literature Cited

(1) Boublikova, L.; Lu, B. C. Y. *J. Appl. Chem.* **1969**, *19*, 89.
(2) Wisniak, J.; Tamir, A. *J. Chem. Eng. Data* **1975**, *20*, 168.
(3) "Selected Values of Properties of Chemical Compounds", *TRC Tables*; Thermodynamic Research Center Data Project: College Station, TX, 1974.
(4) Tsonopoulos, C. *AIChE J.* **1974**, *20*, 263.
(5) Tsonopoulos, C. *AIChE J.* **1975**, *21*, 827.
(6) Wisniak, J.; Tamir, A. *Chem. Eng. Sci.* **1975**, *30*, 335.
(7) Wisniak, J. *Indian J. Technol.* **1984**, *22*, 77.

Received for review July 3, 1986. Revised manuscript received January 29, 1987. Accepted March 26, 1987. This project was partially financed by Bromine Compounds Ltd., Beer-Sheva.

Ultrasonic Velocity, Adiabatic Compressibility, Apparent Molar Volume, and Apparent Molar Compressibility Properties of Ternary Mixtures Containing 2-Butoxyethanol, Water, and Benzene or Decane

N. Prabhakara Rao[†] **and Ronald E. Verrall***

Department of Chemistry, University of Saskatchewan, Saskatoon, Saskatchewan, Canada S7N 0W0

Ultrasonic velocities and densities were measured in ternary systems of 2-butoxyethanol–water–benzene and 2-butoxyethanol–water–decane as a function of composition. Adiabatic compressibility coefficients, excess adiabatic compressibility coefficients, apparent molar volumes, and apparent molar compressibilities were calculated from these data. Transitions from the single-phase region to the two-phase region were found to be continuous with respect to the above properties. The results indicate that the addition of benzene or decane affects the 2-butoxyethanol–water ("clathrate-like") structures observed in binary systems. Increased compressibilities were observed in certain regions of low concentrations of hydrocarbon and water where oil-in-water and water-in-oil microphases, respectively, are present. ^{1}H NMR experiments appear to confirm the presence of water-in-oil microphases.

Introduction

Alcohol and water mixtures show minima and maxima in their thermodynamic properties at low alcohol concentrations (*1*–*7*). It is believed that processes similar to micellization can occur in aqueous solutions of long hydrocarbon chain alcohols. "Clathrate-like" structures of alcohol and water also have been proposed at low concentrations of alcohol. At higher alcohol concentrations merged clathrate structures and aggregates of alcohols have been shown to occur (*4*, *8*, *9*). The presence of a hydrocarbon component can cause changes in these aggregates of water and alcohol sometimes leading to the inclusion of the hydrocarbon in the aggregates. Evidence for the hydrocarbon converting the clathrate-like structures into stable microphases has been observed (*10*–*13*). The characteristic features of these microphases are similar to those of microemulsions which occur in the presence of surfactant. Here the surfactant is believed to stabilize the microphases and thus aid in the formation of microemulsions (*14*).

The ultrasonic velocity, adiabatic compressibility coefficient, and excess adiabatic compressibility coefficient are being studied in order to determine how sensitive they are to pre-

---

[†] On leave from the Department of Physics, Sri Venkateswara University Post Graduate Centre, Kavali 524 202, India.

0021-9568/87/1732-0295$01.50/0

dicting changes in the degree of aggregation in hydrogen bonding liquid mixtures. It is anticipated that these data may provide some evidence for the formation and transformation of microphases in ternary systems of alcohol–water–oil. As well, the apparent molar volume and apparent molar compressibility coefficient properties can be calculated and interpreted in terms of changes induced in the solvent by the solute. In the present work all the above properties of ternary systems of water–2-butoxyethanol–benzene and water–2-butoxyethanol–decane are reported. Also, high-resolution ^{1}H NMR (nuclear magnetic resonance) results are presented for the system containing water–2-butoxyethanol–decane. A detailed discussion of the results of our studies of the binary systems consisting of water–2-butoxyethanol, 2-butoxyethanol–benzene, and 2-butoxyethanol–decane, at different temperatures, are presented elsewhere (*15*).

Experimental Section

Ultrasonic velocities were measured at 25 ± 0.01 °C with a NUSONIC (Mapco, Model 6080) velocimeter operating at 4 MHz. The details of the apparatus and experimental procedure have been presented previously (*15*). The estimated error in the measurement of ultrasonic velocity is ±0.02 m s^{-1}. The solution densities were measured with a SODEV flow densimeter (Model 02D) and they are reproducible to 3 parts in 10^6 (*15*, *16*).

***Materials*.** Spectral grade benzene (BNZ) (BDH) and decane (DEC) (Aldrich) were used without further purification. Water (W) was obtained from a Millipore Super-Q system. 2-Butoxyethanol (BE) (Aldrich) was further purified by fractional distillation under high vacuum and kept over molecular sieves. The final purity was checked with a Tracor 222 gas chromatograph with FID/ECD detector having a glass column packed with 10% Carbowax 20M on 100/120 mesh Supelcoport. No other organic impurities were detected with this unit. The water content of the purified alcohol was estimated by using Karl Fischer titration and found to be <0.03 wt % and was accounted for when solutions with water were prepared.

Results and Discussion

The adiabatic compressibilities, β, in units of bar^{-1} were calculated from the relation $\beta = 100/u^2d$, where u is the ultrasonic velocity in units of m s^{-1} and d is the solution density in g cm^{-3}. The excess adiabatic compressibility coefficients, $\Delta\beta$, were calculated (*17–20*) from the relations

$$\Delta\beta = \beta^{\text{real}} - \beta^{\text{ideal}} \qquad (1)$$

$$\beta^{\text{ideal}} = \sum\phi_i[\beta_i + TV_i\alpha_i^2/C_{p,i}] - T[\sum X_iV_i][\sum\phi_i\alpha_i]^2/[\sum X_i,C_{p,i}] \qquad (2)$$

where ϕ_i, β_i, V_i, α_i, and $C_{p,i}$ are the volume fraction, adiabatic compressibility coefficient, molar volume, coefficient of thermal expansion, and heat capacity at constant pressure, respectively, of the pure component i. T is the absolute temperature.

The apparent molar volume ($\phi_{V,A}$) and apparent molar compressibility ($\phi_{K,A}$) of any solute component A in a solution are given by

$$\phi_{V,A} = M_0(X_0/X_Add_0)(d_0 - d) + M_A/d \qquad (3)$$

$$\phi_{K,A} = \beta\phi_{V,A} + X_0M_0(\beta - \beta_0)/(X_Ad_0) \qquad (4)$$

where d_0, X_0, and β_0 are the density, mole fraction, and adiabatic compressibility coefficient of the solvent, respectively; M_0 is the relative molar mass of the solvent mixture (in the present case containing two components, 1 and 2) and is given by $M_1X_1 + M_2X_2$; X_A and M_A are the mole fraction and relative molar mass of the solute component; d and β are the density and adiabatic compressibility coefficient of the solution mixture, respectively.

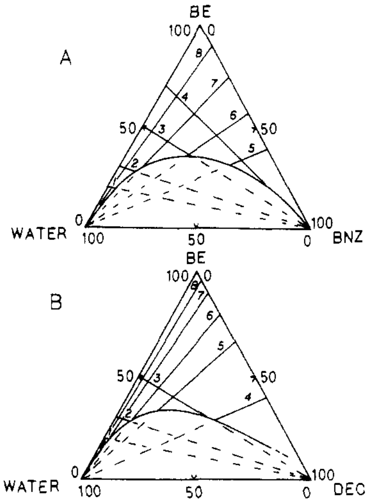

Figure 1. (A) Approximate phase diagram of the system BE–water–BNZ represented in mole percentage; The lines 1–4 and 5–8 represent constant mole ratios of BE/water and BE/BNZ, respectively. (B) Approximate phase diagram of the system BE–water–DEC represented in mole percentage; The lines 1–3 and 4–8 represent constant mole ratios of BE/water and BE/DEC, respectively. T = 25 °C.

The measured data and calculated properties of all systems investigated are found in the supplementary material (see the paragraph at the end of the text regarding supplementary material).

Systems consisting of BE–water–BNZ and BE–water–DEC form two liquid phases at low BE concentrations and at higher concentrations of water and BNZ or DEC. The phase diagrams of these two ternary systems are shown in Figure 1, A and B. The approximate one phase–two phase boundary is represented as a solid curve (*21*, *22*). In order to study these systems it is appropriate to fix the mole ratio of two of the components and to vary the concentration of the third component. Hence, the measurements were made keeping the mole ratio of either BE/water or BE/hydrocarbon constant while varying the concentration of the third component. The straight lines in Figure 1A,B denote the mole ratios of the fixed components and the path along which the concentration of either water or hydrocarbon is varied. A few data points for fixed mole ratio of water/hydrocarbon in the single-phase region were obtained by interpolating the data obtained for fixed BE/water and BE/hydrocarbon conditions. In this paper $X_{BE,DEC}$, $X_{BE,BNZ}$, and $X_{BE,W}$ refer to the mole fraction of BE in the binary mixtures BE + DEC, BE + BNZ, and BE + water, respectively. X_{BE}, X_{BNZ}, X_{DEC}, and X_W refer to the mole fraction content of BE, BNZ, DEC, and water, respectively, in their corresponding ternary systems.

Typical plots of the variation of ultrasonic velocity and adiabatic compressibility coefficient with concentration of BNZ, along lines 1–4 in Figure 1A, are shown in Figures 2 and 3. For fixed mole ratio of BE/water, a monotonic variation of u and β is observed along each line with the value of u decreasing and that of β increasing with increasing BNZ concentration. These changes are greatest at lower concentrations of alcohol, i.e., at lower mole ratio of BE/water.

It is postulated that clathrate-like structures exist in BE–water systems at lower concentration of alcohol (*6*, *8*, *9*), i.e., at a mole fraction of BE ca. 0.015. Beyond this composition, increasing concentration of BE leads to a breakdown of these clathrate-like structures and results in their merging to form BE–water aggregates of different composition. In the ternary systems all of these predicted aggregates of BE–water are likely to be present and one must interpret how the addition of a

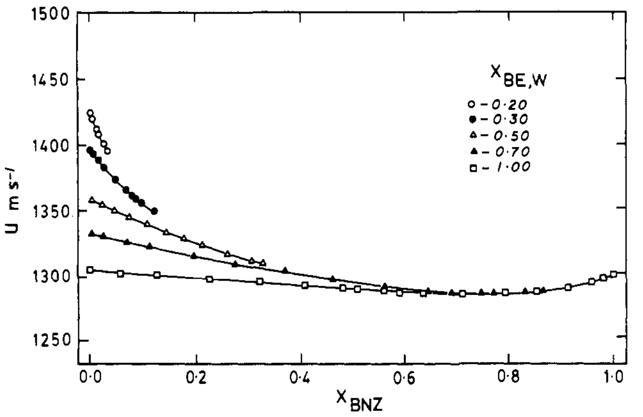

Figure 2. Mixtures of BE-water-BNZ: variation of ultrasonic velocity with concentration of BNZ at different mole fractions of BE in water. $T = 25$ °C.

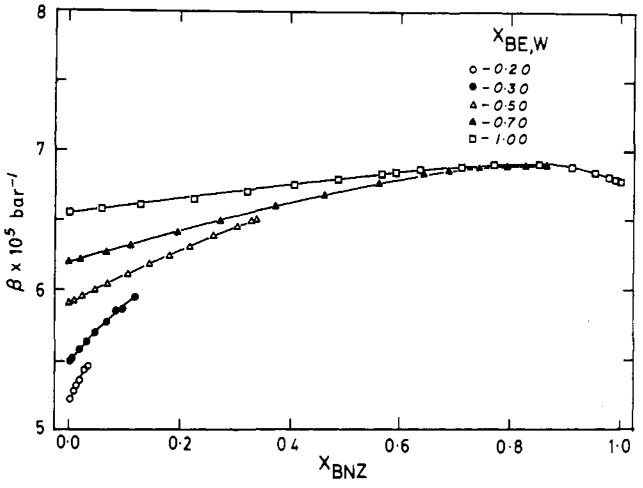

Figure 3. Mixtures of BE-water-BNZ: variation of adiabatic compressibility coefficient with concentration of BNZ at different mole fractions of BE in water. $T = 25$ °C.

hydrocarbon affects them. Qualitatively, the sharp drop in ultrasonic velocity (Figure 2) and steep rise in compressibility coefficient (Figure 3) with increasing BNZ concentration may be interpreted as showing that BNZ is affecting the binary BE-water systems by inducing more intimate contact between BE and BNZ and resulting in the transformation of the binary system aggregates into microphases which resemble oil-in-water microemulsions. These systems are loosely packed and of high compressibility. At higher mole fractions of BE in water, the population of clathrate-like structures is very small, or nil, and the solution properties can be considered from the viewpoint of the interstitial solubilization of BNZ in hydrogen-bonded aggregates of BE (*15*). These two effects are responsible for the broad minimum in the ultrasonic velocity and maximum in the compressibility coefficient at higher BE/water mole ratios.

The decrease in ultrasonic velocity with increasing DEC concentration (Figure 4) is much more abrupt in the case of BE-water-DEC than for BE-water-BNZ. This indicates that DEC has a much greater effect on the clathrate-like structures of BE-water. Correspondingly, the compressibility coefficient sharply increases with increasing DEC concentration. Also, it has been observed that the small addition of DEC to pure BE affects the hydrogen-bonded (self-associated) BE structures (*15*) more than does small additions of BNZ. It is to be noted that the ultrasonic velocity of pure DEC is lower and the compressibility coefficient higher compared to pure BNZ. This fact may be partially responsible for the differences in the behavior of these properties in ternary systems containing BNZ and DEC. However, it is speculated that microphases occur in the single-phase regions of both of these ternary systems and that they are more compressible for systems containing DEC as compared to BNZ.

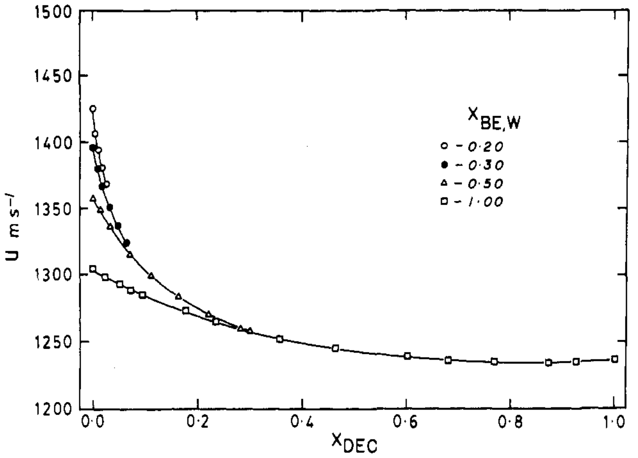

Figure 4. Mixtures of BE-water-DEC: variation of ultrasonic velocity with concentration of DEC at different mole fractions of BE in water. $T = 25$ °C.

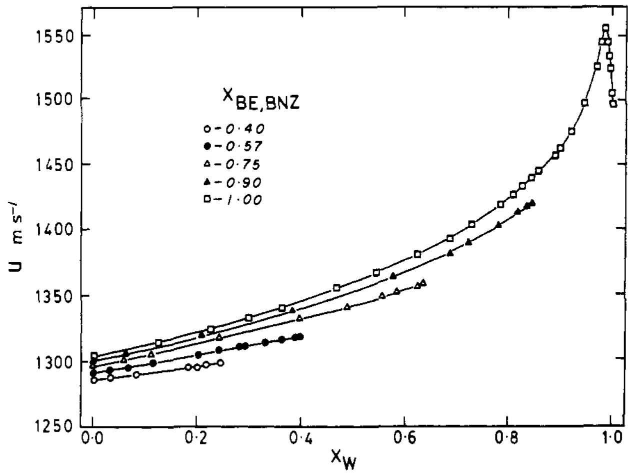

Figure 5. Mixtures of BE-water-BNZ: variation of ultrasonic velocity with concentration of water at different mole fractions of BE in BNZ. $T = 25$ °C.

The curves (Figure 2) showing the variation of ultrasonic velocity in the single-phase region at different mole ratios of BE/water appear to join smoothly with the curves for the binary BE-hydrocarbon system. With stirring, it has been possible to obtain the ultrasonic velocity at concentration conditions extending into the two-phase region where the solutions appear turbid. These velocity values appear to be continuous across the single-phase-two-phase boundary indicating that the transition from the single-phase to the two-phase region is continuous with respect to ultrasonic velocity and adiabatic compressibility properties. Similar conclusions were made with respect to heat capacities in the systems of 2-propanol-water-benzene (*12*). This may indicate that the precursors of droplets that appear as a distinct phase in the 2-phase region are already present in the 1-phase region but are not observable as a distinct phase. In other words, microphase droplets may be developing in the 1-phase region well before the occurrence of 2-phase separation.

In systems of BE-water-BNZ, at fixed mole ratios of BE/BNZ, a regular increase in the ultrasonic velocity (Figure 5) and a regular decrease in adiabatic compressibility coefficient with addition of water is observed along lines 5-8 in Figure 1A. A divergence of these curves is observed at higher concentrations of water, i.e., as the two-phase boundary is reached. The slope of these curves is less at low mole ratios of BE/BNZ, i.e., at

Table I. Molar Volumes, Adiabatic Compressibilities, Coefficients of Thermal Expansion, Molar Heat Capacities at Constant Pressure for the Pure Component Liquids (Used in Eq 2)

	T, °C	V, cm^3 mol^{-1}	$\beta \times 10^5$, bar^{-1}	$\alpha \times 10^3$, K^{-1}	C_p, J K^{-1} mol^{-1}
water	25	18.05	4.477	0.2572^a	75.23^a
	40	18.14	4.312	0.3853	75.21
BE	25	131.78	6.550	0.8541^b	270.60^b
	40	133.71	7.181	0.9274	281.50
BNZ	25	89.43	6.783	1.2422^c	135.80^{c,d}
	40	91.11	7.727	1.2565	138.25
DEC	25	196.00	9.043	1.0286^c	318.95^{c,e}

[a] Reference *23*. [b] Reference *24*. [c] Reference *25*. [d] Reference *26*. [e] Reference *22*.

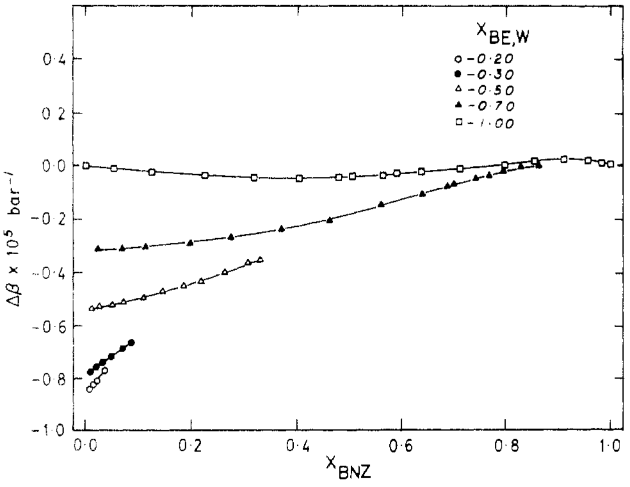

Figure 6. Mixtures of BE-water-BNZ: variation of excess adiabatic compressibility coefficient with concentration of BNZ at different mole fractions of BE in water. T = 25 °C.

lower BE concentrations. This may be interpreted as showing the presence of highly compressible microphases at lower mole ratios of BE/hydrocarbon. The apparent molar specific heat data of BE-water-DEC systems show that hydrocarbon molecules are essentially in contact with BE in this region (*22*). This suggests that the microphases are water-rich droplets dispersed in a benzene-rich continuous phase resembling water-in-oil microemulsions, with BE occupying the interfacial region between water and the hydrocarbon. Such types of water-in-oil microphases also have been proposed from NMR studies of similar systems (*11*). For the systems BE-water-DEC under conditions of fixed mole ratios of BE/DEC and with varying water concentration, the graphs of the ultrasonic velocity and adiabatic compressibility coefficient vs. X_W are similar to those of BE-water-BNZ except that in the former case, the magnitude of these properties is more dependent on the mole ratio of BE/hydrocarbon.

The excess adiabatic compressibility coefficients ($\Delta\beta$) were calculated by using eq 1 and 2. The constants used in eq 2 along with their sources are given in Table I. The variation in values of $\Delta\beta$ for fixed mole ratios of BE/water and BE/hydrocarbon are shown in Figures 6-9 The negative values of $\Delta\beta$ indicate that there is more effective space filling in the multicomponent mixture than there is in the pure components. This feature is more apparent in the systems containing BNZ, the negative values of these systems being greater than in the case of systems containing DEC (cf. Figures 6 and 7 with 8 and 9). BNZ is slightly soluble in water, and in the low-concentration region, though the ultrasonic velocity of BNZ is lower than water, small additions of BNZ to water increase the ultrasonic velocity values above that of pure water. This leads to a reduction in the solution compressibiity and can be viewed as arising from the interstitial accommodation of BNZ within the hydrogen-bonded water aggregates.

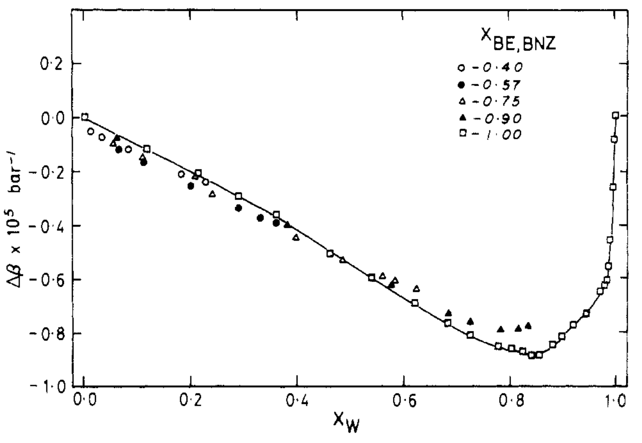

Figure 7. Mixtures of BE-water-BNZ: variation of excess adiabatic compressibility coefficient with concentration of water at different mole fractions of BE in BNZ. T = 25 °C.

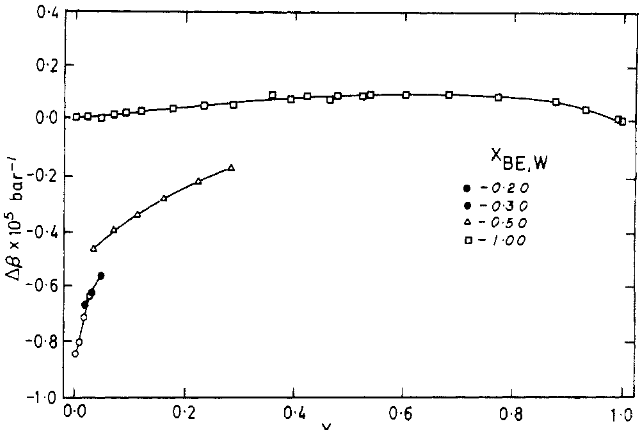

Figure 8. Mixtures of BE-water-DEC: variation of excess adiabatic compressibility coefficient with concentration of DEC at different mole fractions of BE in water. T = 25 °C.

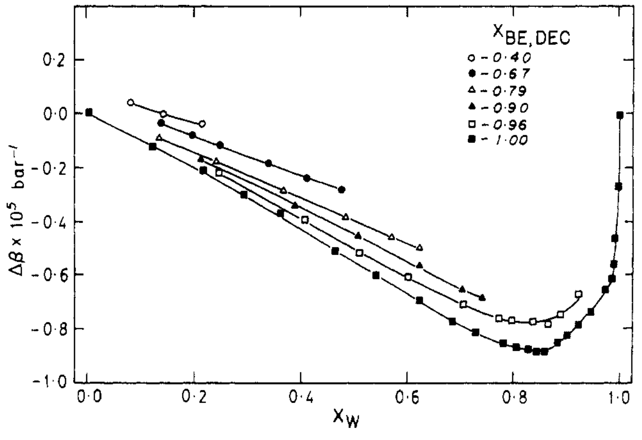

Figure 9. Mixtures of BE-DEC-water: variation of excess adiabatic compressibility coefficient with concentration of water at different mole fractions of BE in DEC. T = 25 °C.

The negative excess adiabatic compressibilities are seen to decrease rapidly with addition of DEC (Figure 8) but decrease more slowly with increasing BNZ composition (Figure 6), at a fixed mole ratio of BE/water. This would appear to support the argument that BNZ is more effective in filling voids in the BE-water aggregates and thus contributes to the low compressibility of the ternary system relative to the pure components. The variation of the values of $\Delta\beta$ with increasing concentration of

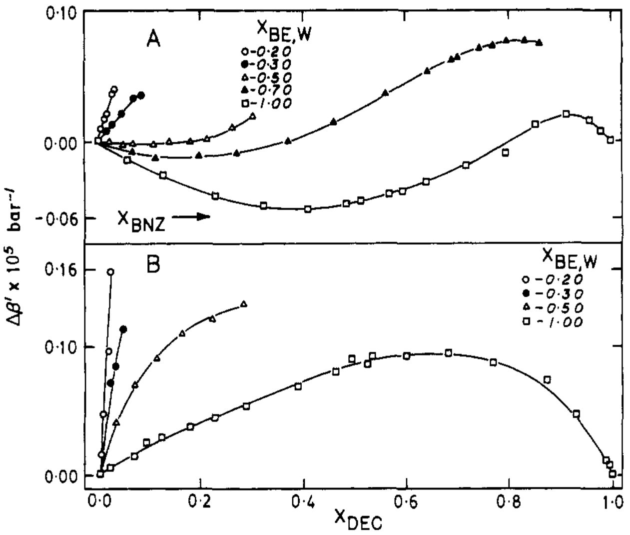

Figure 10. Mixtures of BE-water-BNZ (A) and BE-water-DEC (B): variation of excess adiabatic compressibility coefficient (calculated considering BE-water as a single solvent) with concentration of BNZ (A) and DEC (B) at different mole fractions of BE in BNZ and BE in DEC, respectively. $T = 25$ °C.

water at fixed mole ratios of BE/BNZ and BE/DEC shows that $\Delta\beta$ is relatively independent of BE/BNZ mole ratios. However, in both systems it can be seen that the magnitude of the negative $\Delta\beta$ values, relative to the BE-water mixture values, tends to decrease with increase of water concentration (Figures 7 and 9), thus reflecting the increasing "bulk" water characteristics of the system. An examination of interpolated $\Delta\beta$ data at fixed mole ratios of water/hydrocarbon shows that the magnitude of $\Delta\beta$ becomes less negative as the mole ratio of water/hydrocarbon decreases. This suggests that solvent rearrangement in the ternary system which leads to a decrease in adiabatic compressibility, relative to the pure components, is largely a manifestation of the interactions between BE and water. Such changes are greater at lower concentrations of BE where the clathrate structures are assumed to exist in the binary system.

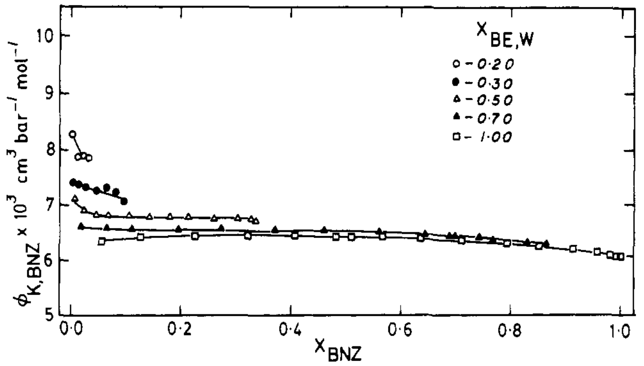

Figure 11. Apparent molar compressibility of BNZ in mixtures of BE-water. $T = 25$ °C.

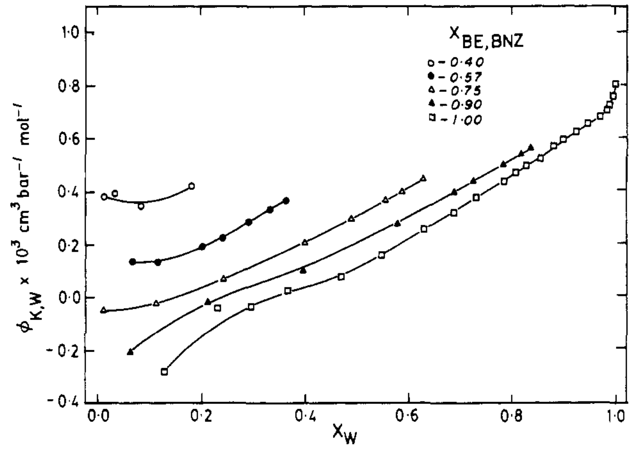

Figure 12. Apparent molar compressibility of water in mixtures of BE-BNZ. $T = 25$ °C.

Treating two of the components in ternary systems as a mixed solvent of fixed composition enables one to study the variation in excess compressibility as a function of the composition of the third component. For example, in systems having fixed mole ratio of BE/water the mixed solvent can be considered as a single component having the physical properties of a BE-water mixture and either BNZ or DEC as the second component. Similarly, BE-BNZ and BE-DEC components at fixed mole ratio can be considered as a mixed solvent and water as the second component. Rather than calculating β^{ideal} (eq 2) as the volume fraction weighted contributions of three components, the ternary system is treated as a pseudobinary system and β^{ideal} is obtained as the volume fraction weighted average of two components where the mixed solvent is treated as a single component. This has the effect of comparing changes in measured solution compressibility with reference to the mixed solvent of fixed mole ratio. The excess compressibility calculated from β^{ideal} obtained by the above procedure is denoted as $\Delta\beta'$ in order to distinguish it from the $\Delta\beta$ previously calculated. For conditions of fixed mole ratios of BE/water and varying compositions of BNZ or DEC, the parameters α and C_p used in the calculation of β^{ideal} for the mixed solvent BE-water were obtained from the literature (*15*, *24*). The variation of $\Delta\beta'$ as a function of BNZ concentration in the pseudobinary systems at different mole fraction of BE-water is shown in Figure 10A. These values represent the excess compressibility considering that the changes can be attributed to the interactions of BE-BNZ, water-BNZ, and to any changes that BNZ causes in BE-water aggregates. Since BNZ (hydrocarbon) is not readily soluble in water, the contribution to $\Delta\beta'$ from the interaction of water-BNZ can be considered as negligible. $\Delta\beta$ data for the binary system BE-BNZ are included also in this figure. The $\Delta\beta'$ values are seen to be higher relative to the binary system and become positive in some cases. The negative values of $\Delta\beta'$ at certain compositions suggest that BNZ is mainly in contact with BE. The positive values of $\Delta\beta'$ suggest, possibly, that there is a breakdown of BE-water aggregates with subsequent formation of microphases upon addition of hydrocarbon. Because there are a number of assumptions implicit in this approach, it is important to note that only the relative changes of $\Delta\beta'$ are meaningful. The differences between the magnitude of $\Delta\beta'$ and $\Delta\beta$ for the systems containing DEC can be seen in Figure 10B. They are greater than the corresponding differences in Figure 10A. This confirms that DEC affects the BE-water solvent system more than BNZ and that the higher compressibility of DEC itself is not the reason for the observed abrupt decrease in ultrasonic velocity and abrupt rise in the compressibility coefficient of systems containing DEC. The specific heat data for the mixed solvents BE-BNZ and BE-DEC were taken as the mole fraction weighted average of the two components. The magnitude of $\Delta\beta'$ calculated by considering BE-BNZ as a pseudo-single-component are the same as $\Delta\beta$ obtained considering all the three components as independent. This is so because the compressibility changes in BE-BNZ systems are relatively small compared to those of BE-water.

The $\phi_{V,BNZ}$, $\phi_{K,BNZ}$, $\phi_{V,DEC}$, and $\phi_{K,DEC}$ properties are found to be virtually invariant with increasing BNZ or DEC concentration. Also, they are independent of the mole ratio of BE/water except at lower concentrations of BNZ or DEC. A typical plot of $\phi_{K,BNZ}$ in BE-water-BNZ mixtures is shown in Figure 11. The $\phi_{K,W}$ values show a strong dependence on the BE concentration in the ternary systems BE-water-DEC and BE-

Table II. Chemical Shifts and Line Widths of the BE Hydroxyl Group Proton Resonance and the Water Proton Resonance

	BE hydroxyl group		water	
X_W	chemical shift, ppm	line width, Hz	chemical shift, ppm	line width, Hz
		$X_{BE,DEC} = 0.300$		
0.0495	4.30	29	3.95	41
0.1354	4.44	41	4.17	47
0.2070	4.45	70	4.30	47
		$X_{BE,DEC} = 0.400$		
0.0533	4.33	35	3.90	53
0.1012	4.53	53	4.18	59
0.2525	4.58	80	4.33	53

water–BNZ. Typical values of $\phi_{K,W}$ as a function of X_W for ternary systems containing BNZ are shown in Figure 12. As in the case of binary BE–water systems (*15*), $\phi_{K,W}$ values in the ternary system also become negative at lower concentrations of water and at higher BE/hydrocarbon mole ratios. The sharp variation of $\phi_{K,W}$ with different mole ratios of BE/hydrocarbon suggests a major change in the environment of water molecules as the BE/hydrocarbon mole ratio changes. This may arise because of the presence of microphases in which water is surrounded by both BE and hydrocarbon and the characteristics of these structures are strongly dependent on the mole ratio of BE/hydrocarbon. Microphases consisting of hydrocarbon surrounded by BE and water are postulated to occur at very low concentrations of hydrocarbon. It appears that the apparent molar compressibility of water in these ternary systems is very sensitive to changing composition and this could have some practical application with respect to assessing the water content in such systems.

The ternary system BE–water–BNZ also was studied at 40 °C. The data obtained are found in the supplementary material. In general, the behavior of the ultrasonic velocity and adiabatic compressibility coefficient are similar to that observed at 25 °C. The slight changes that are seen in the shapes of the curves of these properties as a function of composition are due mainly to the differences between the individual component properties at 25 and 40 °C. However, at 40 °C it was observed at higher mole ratios of BE/BNZ that the variation of these properties is small. The apparent molar volumes and apparent molar compressibilities of BNZ in mixtures of BE–water at 40 °C are greater compared to the values at 25 °C. On the other hand, the apparent molar compressibilities of water in mixtures of BE–BNZ decrease with increasing temperature. The values of $\phi_{K,W}$ at higher mole ratios of BE/BNZ are lower than the values of the binary system BE–water. This means that at higher temperatures the presence of small amounts of BNZ appears to make the environment of water molecules less compressible.

In an attempt to obtain supporting evidence for the presence of water-in-oil microphases at conditions of fixed mole ratios of BE/hydrocarbon and higher compositions of water, the system BE–DEC–water was studied at $X_{BE,DEC} = 0.3$ and 0.4 by using ^1H NMR. Recent studies (*11*, *27–30*) have utilized this technique to investigate water-in-oil microphases and microemulsions in ternary and quaternary (containing surfactant) systems, respectively. Desrosiers et al. (*31*) also have carried out an extensive study of the chemical shifts and relaxation times in BE–D_2O systems by using ^{13}C and ^2H NMR. A Bruker (Model AM-300) NMR spectrometer was used to obtain chemical shifts and line widths at half-height. Tetramethylsilane was used as an external standard. The error in the estimation of chemical shifts is ca. ±0.01 ppm. The chemical shifts and line widths of the BE hydroxyl group proton and water proton resonances at different compositions of water are given in Table II. For both 0.3 and 0.4 $X_{BE,DEC}$ the resonance peaks shift downfield with increasing water content. This shift implies that both the BE hydroxyl group and water protons are being deshielded as the concentration of water is increased. The deshielding of water protons may indicate an increase in the relative degree of water–water hydrogen bonds. The deshielding of the hydroxyl group proton may arise because of the increase in the alcohol–water hydrogen bonding. The data in Table II indicate that the downfield shift of the water proton occurs more rapidly with increasing water concentration compared to that of the hydroxyl group proton of BE. This behavior is consistent with the view that greater water–water interactions occur with increasing water content and hence with increasing water droplet size. Similar results were obtained by Keiser et al. (*11*) in systems of 2-propanol–hexane–water. The line widths of the proton resonance of the hydroxyl group of BE is observed (Table II) to increase with increasing water concentration at both 0.3 and 0.4 $X_{BE,DEC}$ implying an increasing rate of proton exchange. This suggests that a transition from ordered hydrogen-bonded aggregates to less ordered microphases may be occurring. The increase in the line widths of the water proton signals with increase in water content is relatively small compared to those of the BE hydroxyl group resonance. The slight decrease in this trend at higher water concentration for $X_{BE,DEC} = 0.4$ may imply that BE–water hydrogen bonding is predominant at higher BE concentrations and water has less "bulk-water" character. On balance, the NMR studies support the conclusions drawn from the ultrasonic velocity and compressibility results.

Conclusions

The sharp decrease in ultrasonic velocity and the increase in adiabatic compressibility coefficient with increase in hydrocarbon concentration in the region of high concentrations of water in water–oil–BE systems appear to coincide with the transformation of BE–water aggregates into oil-in-water microphases. The increase in the magnitude of the adiabatic compressibility coefficient property, relative to that of the binary mixture BE–water, with increasing water concentration indicates the possible presence of water-in-oil microphases at lower mole ratios of BE/hydrocarbon. Microphases appear to have higher compressibility than the bulk solution with microphases containing DEC, being more compressible than those containing BNZ. The ^1H NMR results support the qualitative arguments drawn from the results of the compressibility studies.

Registry No. BNZ, 71-43-2; BE, 111-76-2; DEC, 124-18-5.

Literature Cited

(1) Franks, F.; Reid, D. J. In *Water-A Comprehensive Treatise*; Franks, F., Ed.; Plenum Press: New York, 1973; Vol. 2, Chapter 5.
(2) Tamura, K.; Mackawa, M.; Yasunaga, T. *J. Phys. Chem.* **1979**, *81*, 463.
(3) Muller, N. *J. Mag. Reson.* **1977**, *28*, 203.
(4) Iwasaki, N.; Fujiyama, T. *J. Phys. Chem.* **1977**, *81*, 1908; **1979**, *83*, 463.
(5) Roux, G.; Roberts, D.; Perron, G.; Desnoyers, J. E. *J. Solution Chem.* **1980**, *9*, 629.
(6) Lara, J.; Desnoyers, J. E. *J. Solution Chem.* **1981**, *10*, 465.
(7) Blandamer, M. J.; Waddington, D. *Adv. Mol. Relaxation Process* **1970**, *2*, 1.
(8) Ito, N.; Saito, K.; Kato, T.; Fujiyama, T. *Bull. Chem. Soc. Jpn.* **1981**, *54*, 991.
(9) Ito, N.; Fujiyama, T.; Udagawa, Y. *Bull. Chem. Soc. Jpn.* **1983**, *56*, 379.
(10) Smith, C. D.; Dorulam, C. E.; Barden, R. E. *J. Colloid Interface Sci.* **1977**, *60*, 488.
(11) Keiser, B. A.; Varie, D.; Barden, R. E.; Holt, S. L. *J. Phys. Chem.* **1979**, *83*, 1276.
(12) Lara, J.; Perron, G.; Desnoyers, J. E. *J. Phys. Chem.* **1981**, *85*, 1600.
(13) Lara, J.; Avedikian, L.; Perron, G.; Desnoyers, J. E. *J. Solution Chem.* **1981**, *10*, 301.
(14) Perron, G.; DeLisi, R.; Davidson, I.; Genereux, S.; Desnoyers, J. E. *J. Colloid Interface Sci.* **1981**, *79*, 432.
(15) Rao, N. P.; Verrall, R. E. *Can. J. Chem.*, submitted for publication.
(16) Picker, P.; Tremblay, E.; Jolicoeur, C. *J. Solution Chem.* **1974**, *3*, 377.
(17) Bertrand, G. L.; Smith, L. E. *J. Phys. Chem.* **1970**, *74*, 4171.
(18) Kiyohara, O.; Benson, G. C. *J. Chem. Thermodyn.* **1979**, *11*, 861.

(19) Benson, G. C.; Kiyohara, O. *J. Chem. Thermodn.* **1979**, *11*, 1061.
(20) Acree, Jr. E. W. *J. Chem. Eng. Data.* **1983**, *28*, 215.
(21) Desnoyers, J. E.; Quirion, F.; Hetu, D.; Perron, G. *Can. J. Chem. Eng.* **1983**, *61*, 672.
(22) Desnoyers, J. E.; Beaudoin, R.; Perron, G.; Roux, G. *ACS Symp. Ser.* **1978**, No. 90.
(23) Kell, G. C. *J. Chem. Eng. Data* **1975**, *20*, 97.
(24) Roux, G.; Perron, G.; Desnoyers, J. E. *J. Solution Chem.* **1978**, *7*, 839.
(25) *International Critical Tables*; McGraw-Hill: New York, 1926.
(26) Fortier, J. L.; Benson, G. C.; Picker, P. *J. Chem. Thermodyn.* **1976**, *8*, 289.
(27) Zlochower, I. A.; Schulman, J. H. *J. Colloid Interface Sci.* **1967**, *24*, 115.
(28) Gillberg, G.; Lehtinen, H.; Friberg, S. *J. Colloid Interface Sci.* **1970**, *40*, 33.
(29) Shah, D. O.; Hamlin, Jr. R. M. *Science* **1971**, *171*, 483.
(30) Hansen, J. R. *J. Phys. Chem.* **1974**, *78*, 256.
(31) Desrosiers, O.; Van Dinter, T.; Saunders, J. K. *Can. J. Chem.* **1984**, *62*, 56.

Received for review July 15, 1986. Accepted March 8, 1987. We thank the Government of Canada and the Government of Saskatchewan for their financial support of this project under the Canada-Saskatchewan Heavy Oil Fossil Fuel Agreement. N.P.R. thanks Sri Venkateswara University for allowing a leave of absence to perform this work.

Supplementary Material Available: Tables of ultrasonic velocity, density, compressibility, and apparent molar properties for various systems (15 pages). Ordering information is given on any current masthead page.

Solubility of Anthracene in Binary Solvent Mixtures Containing Dibutyl Ether

Mary V. Marthandan and William E. Acree, Jr.*

Department of Chemistry, Kent State University, Kent, Ohio 44242

Experimental solubilities are reported for anthracene in binary solvent mixtures containing dibutyl ether with *n*-hexane, cyclohexane, *n*-heptane, methylcyclohexane, *n*-octane, isooctane, and cyclooctane at 25 °C. Results of these measurements, combined with estimates for the excess Gibbs free energies of the binary solvents, are used to test predictive expressions derived from the nearly ideal binary solvent (NIBS) model. Expressions based on a volume fraction average of solute properties in the two pure solvents predict anthracene solubilities to within a maximum deviation of 5.1% and an overall average deviation of 2.1%.

Introduction

This work continues (*1–8*) a systematic search for mixing models and equations which will provide predictions for thermochemical properties of a solute at high dilution in binary solvent mixtures. In two earlier papers, Acree and Rytting (*5*, *6*) reported solubilities for benzil and *p*-benzoquinone in binary solvent mixtures containing carbon tetrachloride, in which the mole fraction solubility of benzil and *p*-benzoquinone cover a 14-fold and 6-fold range, respectively. The experimental data were interpreted with solution models developed previously for solubility in systems containing specific solute–solvent interactions and with models of purely nonspecific solute–solvent interactions and with models of purely nonspecific interactions. A stoichiometric complexation model based entirely on specific interactions (nonspecific interactions ignored) required several equilibrium constants to mathematically describe the experimental results, while the nearly ideal binary solvent (NIBS) model based on nonspecific interactions described adequately the observed solubilities without introducing a single equilibrium constant.

The success of the NIBS approach in predicting the binary solvent effect on benzil and *p*-benzoquinone solubilities suggested the possibility that this solution model may provide a foundation for approximations of physical interactions even in a system known to contain chemical interactions. To pursue this idea further, the basic NIBS model was extended to systems containing association between the solute (component A) and a complexing cosolvent (component C)

$$\mathrm{A_1} + \mathrm{C_1} \rightleftharpoons \mathrm{AC}$$

$$K_{\mathrm{AC}}{}^{\phi} = \frac{\phi_{\mathrm{AC}}}{\phi_{\mathrm{A_1}}\phi_{\mathrm{C_1}}}$$

A relatively simple expression was developed (*8*) for the determination of solute–solvent equilibrium constants from the measured solubility as a function of solvent composition and the excess Gibbs free energy of the binary solvent mixture

$$RT\left[\ln\left(a_{\mathrm{A}}{}^{\mathrm{solid}}/\phi_{\mathrm{A_1}}{}^{\mathrm{sat}}\right) - 1 + \bar{V}_{\mathrm{A}}\left(\frac{\phi_{\mathrm{A_1}}{}^{\mathrm{sat}}}{\bar{V}_{\mathrm{A}}} + \frac{\phi_{\mathrm{B}}}{\bar{V}_{\mathrm{B}}} + \frac{\phi_{\mathrm{C}}}{\bar{V}_{\mathrm{C}}}\right)\right] = (1 - \phi_{\mathrm{A}}{}^{\mathrm{sat}})^2[\phi_{\mathrm{B}}{}^0(\Delta\bar{G}_{\mathrm{A}}{}^{\mathrm{fh}})_{\mathrm{B}}{}^* + \phi_{\mathrm{C}}{}^0(\Delta\bar{G}_{\mathrm{A}}{}^{\mathrm{fh}})_{\mathrm{C}}{}^* - \bar{V}_{\mathrm{A}}(X_{\mathrm{B}}{}^0\bar{V}_{\mathrm{B}} + X_{\mathrm{C}}{}^0\bar{V}_{\mathrm{C}})^{-1}\,\Delta\bar{G}_{\mathrm{BC}}{}^{\mathrm{fh}}] \quad (1)$$

with the overall volume fraction solubility, $\phi_{\mathrm{A}}{}^{\mathrm{sat}}$, being related to the solubility of the *uncomplexed* solute and the equilibrium constant by

$$\phi_{\mathrm{A}}{}^{\mathrm{sat}} = \phi_{\mathrm{A_1}}{}^{\mathrm{sat}}[1 + \bar{V}_{\mathrm{A}}K_{\mathrm{AC}}{}^{\phi}\phi_{\mathrm{C_1}}/(\bar{V}_{\mathrm{A}} + \bar{V}_{\mathrm{C}})]$$

and the quantities $(\Delta\bar{G}_{\mathrm{A}}{}^{\mathrm{fh}})_{\mathrm{B}}{}^*$ and $(\Delta\bar{G}_{\mathrm{A}}{}^{\mathrm{fh}})_{\mathrm{C}}{}^*$ being calculated from the appropriate binary reduction of eq 1

$$(\Delta\bar{G}_{\mathrm{A}}{}^{\mathrm{fh}})_{\mathrm{B}}{}^* = (1 - \phi_{\mathrm{A}}{}^{\mathrm{sat}})^{-2}RT\left[\ln\left(a_{\mathrm{A}}{}^{\mathrm{solid}}/\phi_{\mathrm{A}}{}^{\mathrm{sat}}\right) - (1 - \phi_{\mathrm{A}}{}^{\mathrm{sat}})\left(1 - \frac{\bar{V}_{\mathrm{A}}}{\bar{V}_{\mathrm{B}}}\right)\right]$$

$$(\Delta\bar{G}_{\mathrm{A}}{}^{\mathrm{fh}})_{\mathrm{C}}{}^* = (1 - \phi_{\mathrm{A}}{}^{\mathrm{sat}})^{-2}RT\left[\ln\left(a_{\mathrm{A}}{}^{\mathrm{solid}}/\phi_{\mathrm{A_1}}{}^{\mathrm{sat}}\right) - 1 + \bar{V}_{\mathrm{A}}\left(\frac{\phi_{\mathrm{A_1}}{}^{\mathrm{sat}}}{\bar{V}_{\mathrm{A}}} + \frac{\phi_{\mathrm{C}}}{\bar{V}_{\mathrm{C}}}\right)\right]$$

using the molar volumes of the pure components, $\bar{V}_{\mathrm{i}}$, and the solubilities in the two pure solvents. The superscript (0) denotes that the solvent compositions are calculated as if the solute were not present.

Postulating the formation of a 1:1 anthracene–benzene complex, the authors demonstrated that eq 1 could describe

0021-9568/87/1732-0301$01.50/0 © 1987 American Chemical Society